
Classic Chest Radiology Findings, Pearls and Pitfalls

Gloria Soto and Karla Moënne

Contents

1	Introduction	13
2	Mediastinum	14
2.1	Size and Shape	14
2.2	Pitfalls and Abnormalities.....	15
3	Abnormal Radiological Density	19
3.1	Technical Pitfalls.....	19
3.2	Chest Wall, Lung, and Pleural Findings	21
4	Conclusion	29
	References	29

Abstract

Chest radiography is the most frequent examination performed in the majority of pediatric radiology departments. It remains the initial imaging study to evaluate most thoracic diseases in children. A systematic approach to the interpretation of children's chest radiographs, knowledge of basic radiological findings, and consideration of clinical information, are the key for a correct radiological diagnosis. Obtaining a technically adequate chest radiograph in small children is particularly challenging due to their lack of cooperation. Potential pitfalls related to suboptimal images have to be considered. Throughout this chapter we will discuss radiological findings of the normal and pathological pediatric chest, including pathologic conditions concerning the chest wall, pleura and lungs, and also some potential technical pitfalls.

1 Introduction

Chest radiography is the most frequent examination performed in most pediatric radiology departments (Frush et al. 2000), representing up to 30–50 % of the total workload (Khun and Effmann 2004). It is the initial imaging study to evaluate the vast majority of thoracic diseases in children (Enríquez et al. 2009).

Correct interpretation of chest radiographs requires trained radiologists and technically adequate images, a special challenge in uncooperative children.

A systematic approach in the interpretation of children's chest radiographs, knowledge of basic radiological findings, and consideration of clinical information, are key factors for a correct radiological diagnosis. On the other hand, failure in adequate interpretation can lead to wrong diagnosis and consequently to inappropriate therapeutic management (Enríquez et al. 2009).

G. Soto (✉)
Departamento de Diagnóstico por Imágenes,
Clínica Alemana de Santiago de Chile,
Vitacura 5951, 8510080, Santiago, Chile
e-mail: gloria.soto@gmail.com

K. Moënne
Departamento de Diagnóstico por Imágenes,
Clínica Las Condes, Lo Fontecilla 441,
7591046, Santiago, Chile

Throughout this chapter we will discuss radiological findings related to:

- Mediastinum
 - Size and shape
 - Pitfalls and pathological conditions
- Abnormalities of radiological density
 - Technical pitfalls
 - Chest wall, lung, and pleural origin.

2 Mediastinum

2.1 Size and Shape

The variable size and shape of the normal mediastinum in children, and even in the same child, constitutes a special challenge in the interpretation of chest radiographs. (Nasseri and Eftekhari 2010).

Different divisions of the mediastinum, for both descriptive and diagnostic purposes, have been proposed in the literature. A simple method that applies to chest radiograph interpretation considers three mediastinal compartments: anterior, middle, and posterior (Fig. 1) (Fraser 1996).

2.1.1 Thymus

Normal mediastinum is particularly prominent in small children due to the characteristic prominent thymus at this age.

The thymus is usually visible in chest radiographs of children under 3 years of age, and occasionally beyond that age. Size and growth pattern of the thymus has been matter of many studies. Classically, it has been considered that the thymus increases in size until puberty, and then involutes progressively. It has also been postulated that its prominence in small children is more related to the smaller body mass of children, rather than to a real absolute large volume. According to a study performed by Steinmann the thymus attains its maximum size during the first few months of life and does not grow any larger beyond that age (Nasseri and Eftekhari 2010).

Normal thymus has soft contours and does not compress adjacent structures. In chest radiographs it has a similar density to the adjacent heart and vascular structures. As a result, delineation of the borders of these structures is difficult and diagnostic errors can occur if the radiologic characteristics of the thymus are not considered.

Three classical radiological signs have been described regarding the radiologic representation of the thymus: (Enríquez et al. 2009; Nasseri and Eftekhari 2010).

- *Wave sign*: wavy contour of the thymus caused by indentation of its soft tissue by the anterior costal arches (Fig. 2).
- *Sail sign*: triangular and usually slightly convex appearance of the right lobe of the thymus delineated inferiorly

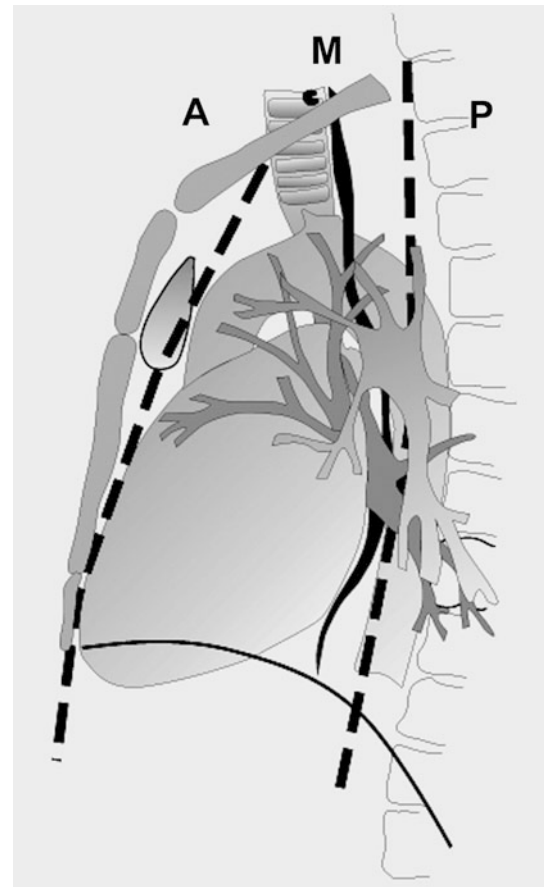


Fig. 1 Diagram of a lateral view of the chest showing the three mediastinal compartments and the anatomic structures they contain. A Anterior compartment, M Medium compartment, and P Posterior compartment (Reprinted with permission from Moënné and Ortega 2012)

by the minor fissure of the right lung (Fig. 3). It is present in approximately 5 % of children and is seen both in frontal and lateral views (Nasseri and Eftekhari 2010).

- *Cardiothymic incisure*: small indentation seen in frontal views in one or both sides of the mediastinum (Fig. 4).

In patients under stress (acute respiratory illness, surgery, steroid therapy, radiotherapy and others), significant decrease in the size of the thymus can be seen, as well as changes in its configuration. Once stress is over, the thymus can grow up to 50 % more of its original size. This “thymic rebound” occurs mainly in children, though it can also be seen in adults (Nasseri and Eftekhari 2010).

It is important to remember the role of ultrasound (US) in characterizing normal thymus parenchyma. In cases of uncertain radiological images, US, using the anterior chest wall as acoustic window, is extremely helpful to identify the thymus and define its participation in mediastinal size and shape (Han et al. 2001).



Fig. 2 The wave sign: note the wavy contour of the thymus on the left side, caused by indentation of its soft tissue by the anterior costal arches

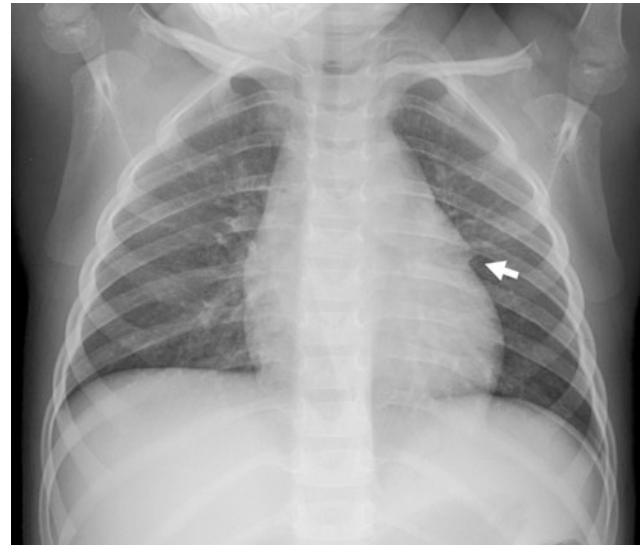


Fig. 4 The cardiophymic incisure: the *arrow* shows a small indentation where the thymus contacts the cardiac border

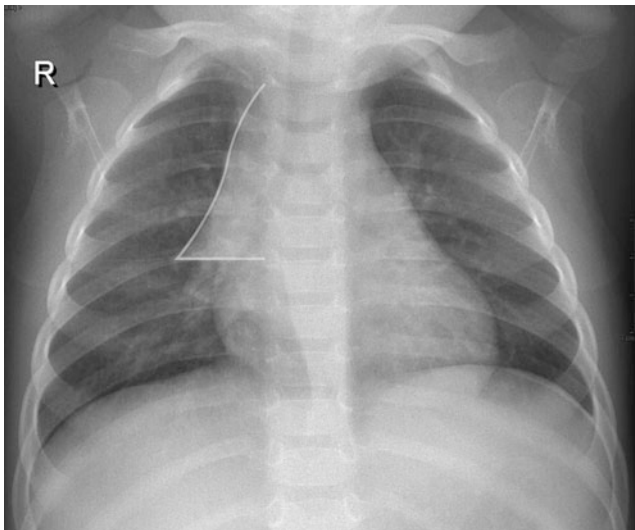


Fig. 3 The sail sign: the right lobe of the thymus has a triangular shape with its inferior border limited by the horizontal fissure of the right lung

2.1.2 Heart

Changes in the size and configuration of the heart can also affect the radiological representation of the mediastinum. When analyzing the heart the position in which the child was examined must be considered. In supine position the heart appears more prominent than in standing position. It is important to remember that a supine frontal view is routinely used in infants, whereas toddlers and older children are generally examined in standing position (Enríquez et al. 2009). Lateral views are useful to evaluate posterior cardiac enlargement and, in absence of a large thymus, right ventricular size by noting the area of contact of the heart with the sternum (Fig. 5a, b).

Frontal views obtained in expiratory phase are a frequent cause of wrong diagnosis of mediastinum widening and heart enlargement (Fig. 6) (Enríquez et al. 2009)

2.1.3 Trachea

The trachea is represented in chest radiographs throughout all its extension, especially when digital technique is used. A careful analysis of the tracheal air column has to be done, both in frontal and lateral views. If a tracheal tube is present, proper position must be confirmed.

In the frontal view the proximal subglottic trachea shows bilateral symmetric convexities, a finding described as “shouldering” of the air column (Fig. 7). Distal to this the diameter of the trachea remains constant and its walls are parallel, except where the aortic arch causes a localized indentation. Occasionally in asymptomatic children an anomalous innominate artery or, less frequently, the common carotid artery can produce an anterior indentation of the trachea at the level of the sternal manubrium. This finding is only seen in small children, in whom there is proportionately less space in the upper mediastinum and therefore a greater possibility that these arteries indent the trachea. A frequent associated finding in these cases is tracheomalacia, believed to be the cause of symptoms, such as stridor and respiratory distress, present in some of these children (Swischuk 1971).

2.2 Pitfalls and Abnormalities

Due to the greater flexibility and relatively larger size of the trachea it is frequent to see in children less than 5 years of age lateral tracheal deviations and even angulations. This finding is more pronounced with cervical flexion and in

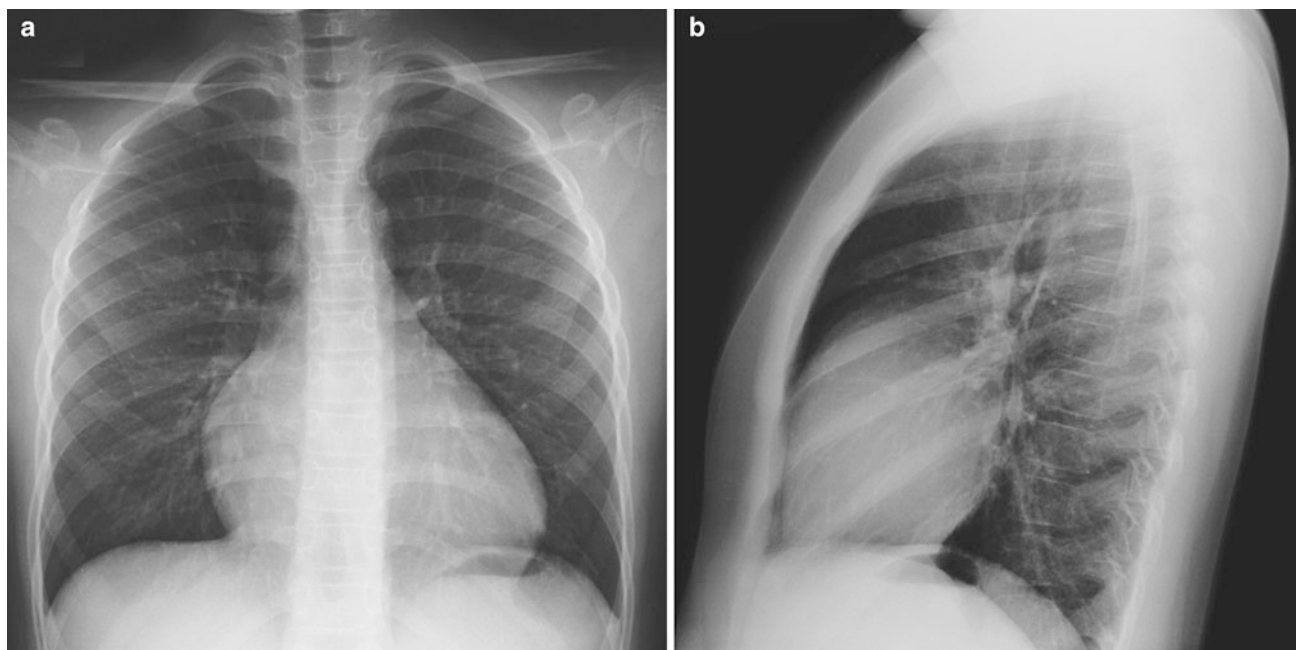


Fig. 5 Frontal chest radiograph of a prominent heart (a). Lateral view shows wide contact of the anterior border of the heart with the sternum, indicating right ventricular enlargement (b)



Fig. 6 Frontal under-inspired chest radiograph of a normal child. Note the apparent widening of the mediastinum and enlargement of the heart. The radiograph was repeated with adequate degree of inspiration and both the mediastinum and the heart showed a normal appearance

under-inspired images (Fig. 8) (Moëne and Ortega 2012). This physiologic tracheal deviation is usually toward the right, opposite direction to the aortic arch, which “anchors” the trachea avoiding lateral deviation toward its side.

Any anterior displacement of the intrathoracic trachea must be considered abnormal (Fig. 9), as well as any lateral deviation in children over 5 years of age (Chang et al. 1970).

Recognizing “physiological” tracheal deviations is important to prevent performing unnecessary studies in healthy children.



Fig. 7 Frontal view of the proximal trachea. Note the bilateral symmetric convexities of the normal subglottic trachea, known as “tracheal shouldering”

When tracheal inflammation is present, underlying edema causes narrowing of the subglottic trachea with loss of the normal tracheal “shouldering” (Fig. 10). The inverted V configuration of the trachea under these circumstances is

Fig. 8 Under-inspired (a) and well-inspired frontal chest radiographs (b) of a 2-year-old boy. Note the right-sided lateral deviation of the trachea that is completely straight in the well-inspired radiograph

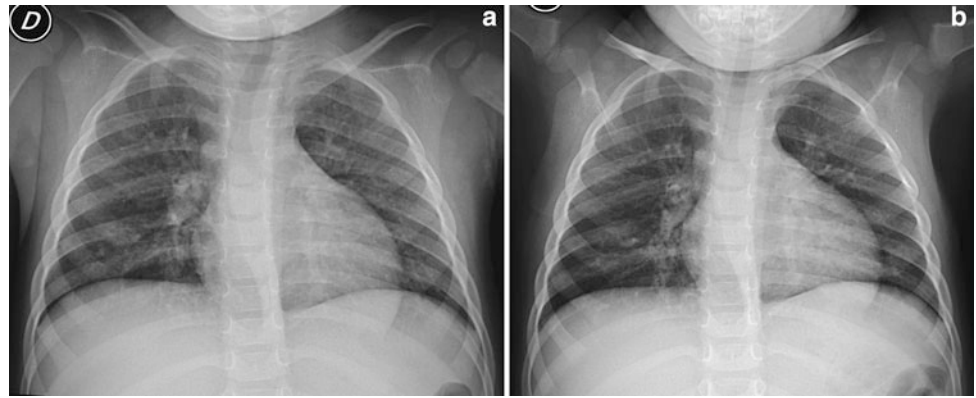


Fig. 9 Lateral chest radiography showing anterior deviation of the trachea (a) secondary to a bronchogenic cyst, demonstrated on CT (b)

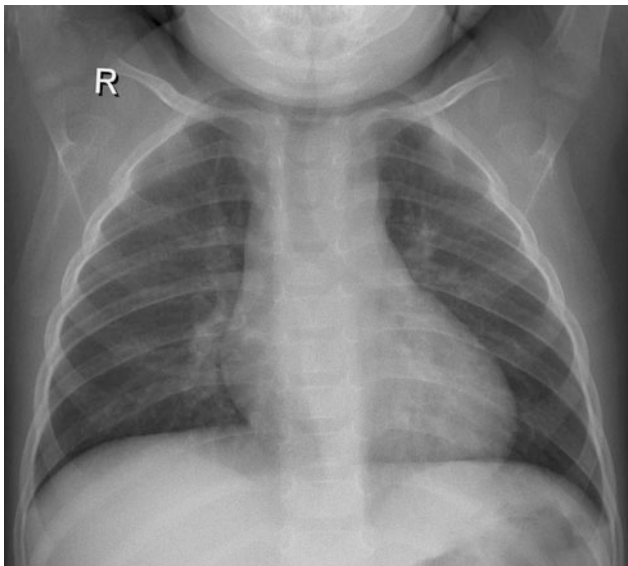
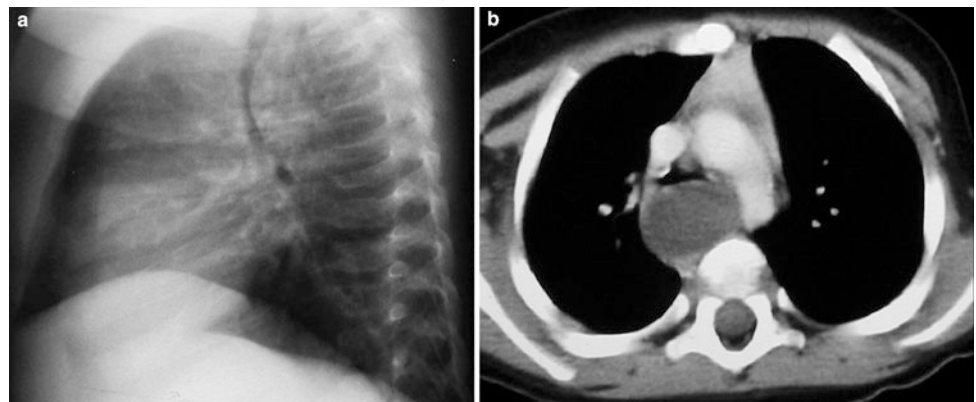


Fig. 10 The steeple sign. Note the inverted V shape of the subglottic trachea representing underlying inflammation and edema in a child with croup. The normal “shouldering” of the trachea at this level is lost

called the *steeple sign*. It is a non-specific sign most frequently caused by croup or laryngotracheobronchitis. Even if the diagnosis of croup is clinical, radiographs may be requested to exclude other causes of stridor, such as foreign

body aspiration, an esophageal foreign body, congenital subglottic stenosis, epiglottitis or a subglottic hemangioma. In these cases the *steeple sign* helps to define croup as the cause of the symptoms (Salour 2000).

Any tracheal indentation or narrowing, other than those previously mentioned, has to be considered abnormal. Diffuse narrowing is usually congenital, due to complete cartilaginous tracheal rings (Fig. 11a, b). Focal narrowing is more frequently a complication of tracheal intubation. Tracheal compressions caused by vascular structures can be detected in radiographs, however CT or magnetic resonance (MR) imaging is mandatory to define the exact vascular anatomy and its relation to the airway. Tracheomalacia, defined as the dynamic collapse of the trachea during the expiratory phase, can be isolated or associated to vascular rings or tracheoesophageal fistula. Stridor and occasionally dyspnea are the clinical manifestations.

Masses, either congenital or tumoral, can originate in any mediastinal compartment. Chest radiographs can show compression or displacement of adjacent structures (Fig. 12), however, their characterization requires imaging with CT or MRI (Zylak et al. 2000).

If a chest radiograph shows signs of mass effect over mediastinal structures, CT or MR studies are mandatory to complete imaging investigation.

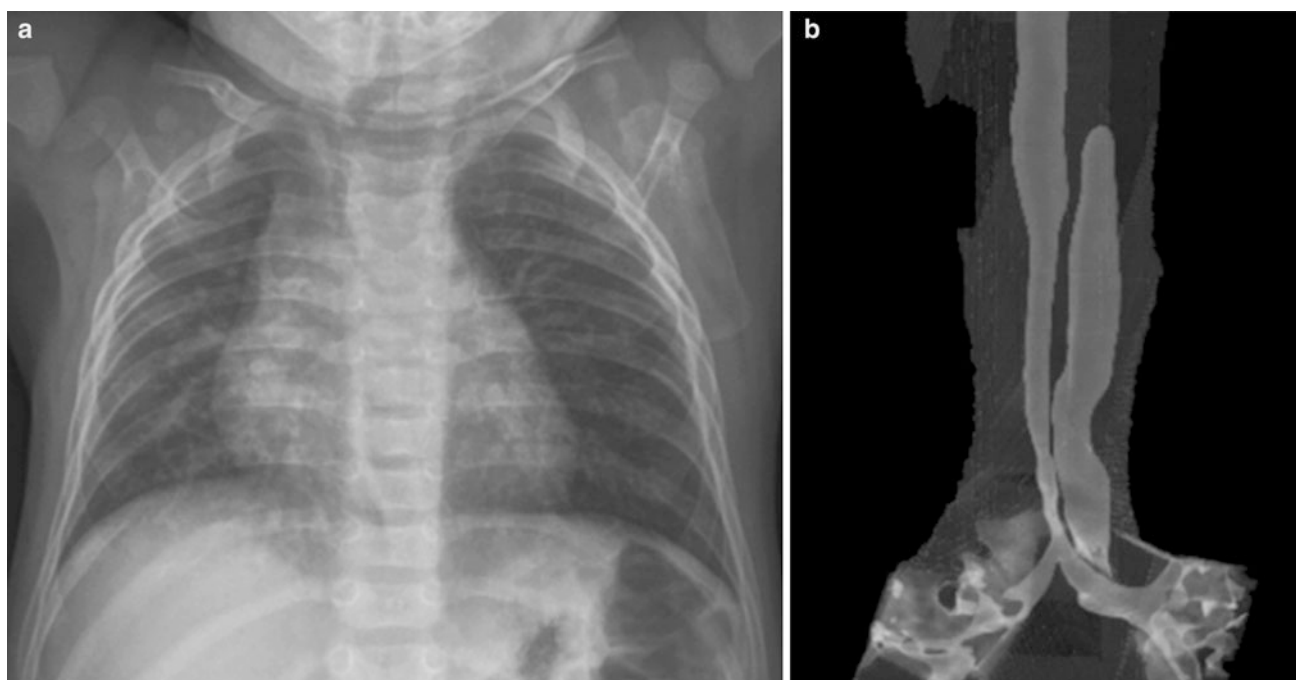


Fig. 11 Frontal chest radiograph (a) and CT coronal volume rendering image of the trachea (b) in a child with type II pulmonary sling. Note the low T-shaped carina and the long segment narrowing of the intrathoracic trachea



Fig. 12 A huge anterior mediastinal mass produces lateral deviation of the heart and trachea. CT showed a mediastinal teratoma

Pneumomediastinum can result from a variety of causes that may be either intra or extrathoracic, and that vary with age (Zylak et al. 2000). While occasionally it can be secondary to intrathoracic spread of air from the cervical region or from the abdomen, most cases are secondary to alveolar over distension and rupture due to high intra-alveolar pressure. (Chalumeau et al. 2001). A variety of conditions have been described in relation to pneumomediastinum in

children, including trauma, medical illnesses, and iatrogenic. Although in some children it may occur spontaneously, a trigger can be found in up to 70–90 % of cases; the most frequent are asthma, vomiting of any cause, situations involving repetitive Valsalva maneuver, and intense sport activities. In newborns respiratory effort can be the sole cause of pneumomediastinum.

Radiographic signs of pneumomediastinum reflect the free air dissecting different anatomic mediastinal structures (Zylak et al. 2000). The main radiological signs in children are:

- *Retrosternal and precardiac hyperlucency*: collection of air in the anterior mediastinum compartment (Fig. 13).
- *Periaortic and peritracheal lucent streaks*: dissection of air into the mediastinum or the mediastinal recesses (Fig. 14).
- *Angel-wing sign, or spinnaker sail sign*: elevation and lateralization of the lobes of the thymus by air in the mediastinum (Fig. 15).
- *Ring around the artery sign*: radiolucent line surrounding the right pulmonary artery, seen on the lateral view (Fig. 16).
- *Continuous diaphragm sign*: interposition of air between pericardium and diaphragm making visible the central part of the diaphragm in continuity with the diaphragmatic domes (Fig. 17).

Indirect signs of pneumomediastinum are *subcutaneous emphysema*, usually present in infants and older children but not in newborns, and *pneumopericardium*.

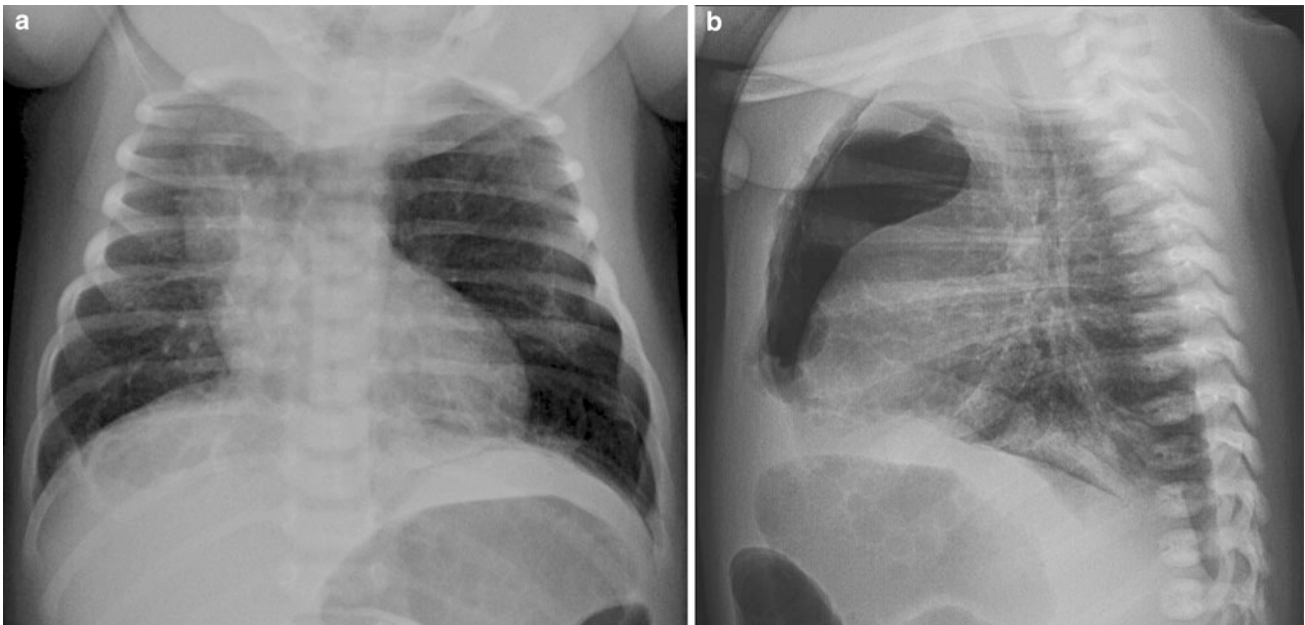


Fig. 13 Pneumomediastinum: a large collection of air is seen in the retrosternal and pre cardiac region of the anterior mediastinum, in frontal (a) and lateral (b) chest views. Note elevation of the thymus lobes

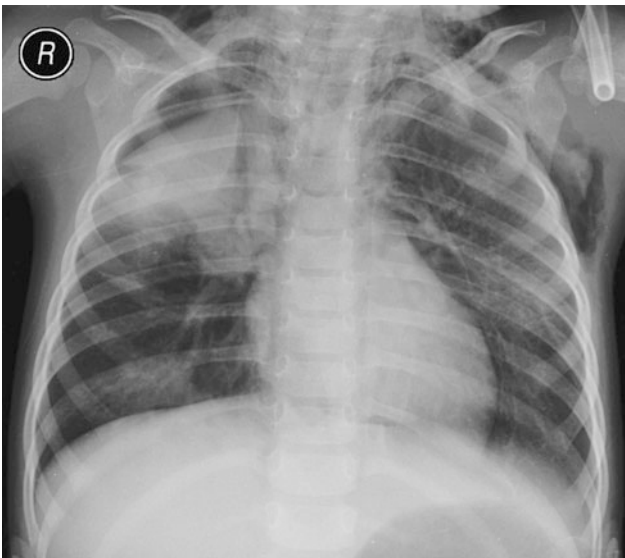


Fig. 14 Frontal chest radiograph in a child with pneumomediastinum and right pneumothorax. Note streaks of air dissecting the upper mediastinal structures. The medial pleural line is also seen as well as subcutaneous emphysema

Pneumomediastinum may be difficult to differentiate from medial pneumothorax; lateral views are useful to differentiate both conditions. In addition, pneumomediastinum may be simulated by the Mach band effect, which corresponds to a lucent band adjacent to convex borders such as the cardiac contour. Identification of a pleural line, which is characteristic of pneumomediastinum, aids in differentiation.

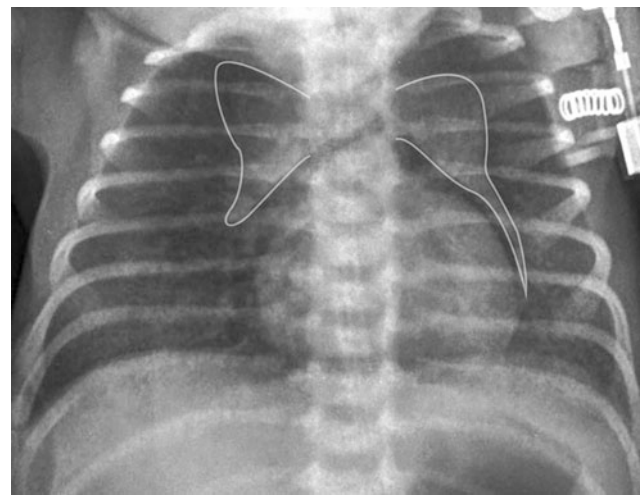


Fig. 15 The “angel sign” elevation and lateralization of both thymic lobes that are separated by air from the adjacent mediastinal structures

3 Abnormal Radiological Density

3.1 Technical Pitfalls

Rotation of the chest is the most frequent cause of an apparent hyperlucent lung. The posterior-most hemithorax looks larger and more lucent than the contra lateral. The best way to assess rotation is measuring the distance between the medial aspect of the anterior costal arches and



Fig. 16 Lateral chest radiograph showing the “ring around the artery sign” in a 15-year-old girl with spontaneous pneumomediastinum. Note the radiolucent line surrounding the right pulmonary artery (arrow)



Fig. 17 Frontal chest radiograph of an infant with pneumomediastinum showing the “continuous diaphragm sign”

the spine, which is symmetrical in the properly positioned child (Fig. 18). Evaluation of clavicular symmetry, a method widely used in adults, is less reliable in children, who can be symmetric in the upper part of the thorax and rotated inferiorly (Fig. 19). Another frequent cause of

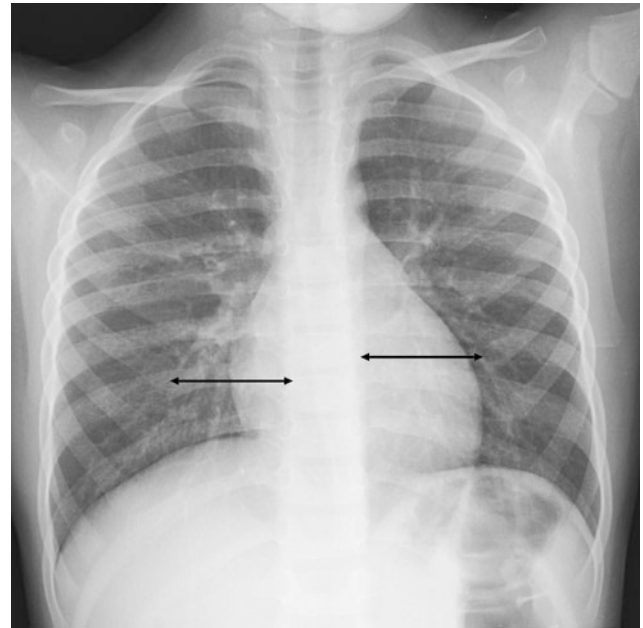


Fig. 18 In a non-rotated frontal chest radiograph the distance between the medial aspect of the anterior costal arches and the spine is symmetric (arrows)

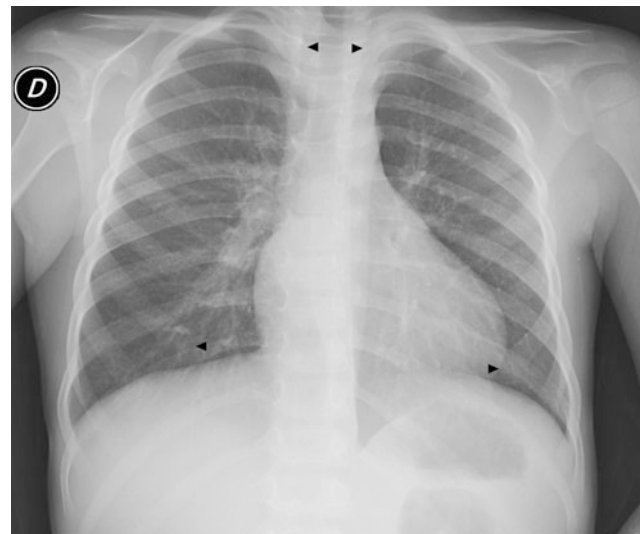


Fig. 19 Frontal chest radiograph showing symmetry at the level of the clavicles (upper arrowheads). Note however the asymmetry in the length of the anterior costal arches in both hemithoraces (lower arrowheads) due to rotation of the inferior thorax

apparent unilateral lung hyperlucency is related to X-ray beam misalignment. Comparative evaluation of the chest wall soft tissues density on both hemithoraces is very useful to identify this technical pitfall since they will display the same asymmetry of transparency as the lungs (Fig. 20).

A poorly inspired film, very frequent in infants and uncooperative children, is another source of diagnostic



Fig. 20 Apparent unilateral lung hyperlucency of the right hemithorax due to X-ray beam misalignment. Note similar asymmetry of the chest wall soft tissues density on both hemithoraces, the right side more lucent than the left

errors. An apparent increase in lung density, poor definition of vessels, and widening of the mediastinum are usual findings in this situation, and can easily be misinterpreted as abnormalities by the inexperienced radiologist. Regarding this topic, Leonard Swischuk, says: “*While many aspects of medicine are scientific, judging the degree of inspiration on a chest film is not in this category and probably never will be*” (Swischuk 1997). Experience, gained with practice, is the key to correctly determine if a radiograph has been obtained with an adequate degree of inspiration. Evaluation by counting the costal arches, or the intercostal spaces, is not always reliable, and, if used as the only parameter can be misleading, especially in infants (Fig. 21a, b). A useful clue is to evaluate the definition of the lung vessels, which are well-defined in adequately inspired films. The configuration of the thoracic cage also helps since in expiratory radiographs usually the transverse diameter predominates over the longitudinal diameter, as opposed to what happens in well-inspired images (Moënné and Ortega 2012).

3.2 Chest Wall, Lung, and Pleural Findings

3.2.1 Chest Wall

Poland syndrome, a rare congenital malformation of the chest wall consisting of hypoplasia or aplasia of the pectoralis major muscle and adjacent cartilaginous, osseous,

and soft tissue structures, causes increased transparency of the affected hemithorax (Fefferman and Pinkney 2005). The clue to establish the diagnosis is comparative analyses of the soft tissues of the chest wall, which are less dense and prominent in the affected side (Fig. 22a, b). Physical examination confirms the diagnosis.

3.2.2 Lung

3.2.2.1 Decreased Lung Density

For a correct diagnostic approach of decreased density (or increase transparency) of one or both lungs, it is important to evaluate lung volume and vascularity.

Three scenarios must be considered when there is diffuse bilateral lung hyperlucency:

- Increased lung volume with normal vascularity
- Normal lung volume with decreased vascularity
- Increased lung volume with decreased vascularity.

3.2.2.2 Increased Lung Volume with Normal Vascularity

Bilateral increase of lung volume with normal vascularity can be physiologic or secondary to diffuse mild obstruction of the small airway. To differentiate both situations, the position and configuration of the hemidiaphragms, and the mediastinal position have to be considered.

As already mentioned it is difficult, if not impossible, to control the respiratory phase in which radiographs are obtained in infants and uncooperative children. If the patient cries during the examination it is possible to obtain images during deep inspiration, showing large hyper lucent lungs. A clue to suspect that a deep inspiration is the cause is the presence of discrepancy of the lung volume in frontal versus lateral views (Fig. 23a, b).

Air trapping due to airway obstruction, as seen in bronchiolitis and asthma, is constant throughout the respiratory cycle, hence diaphragmatic flattening is present in both frontal and lateral views (Bramson 2005) (Fig. 24a, b). In these cases an increase of retrosternal air is usually seen in the lateral view. Decreased lung vascularity could be found in severe cases.

To diagnose air trapping, the diaphragm needs to be flattened on both frontal and lateral views.

3.2.2.3 Normal Lung Volume with Decreased Vascularity

When a child has normal-sized hyperlucent lungs with decreased vascularity, a cardiovascular disease, such as

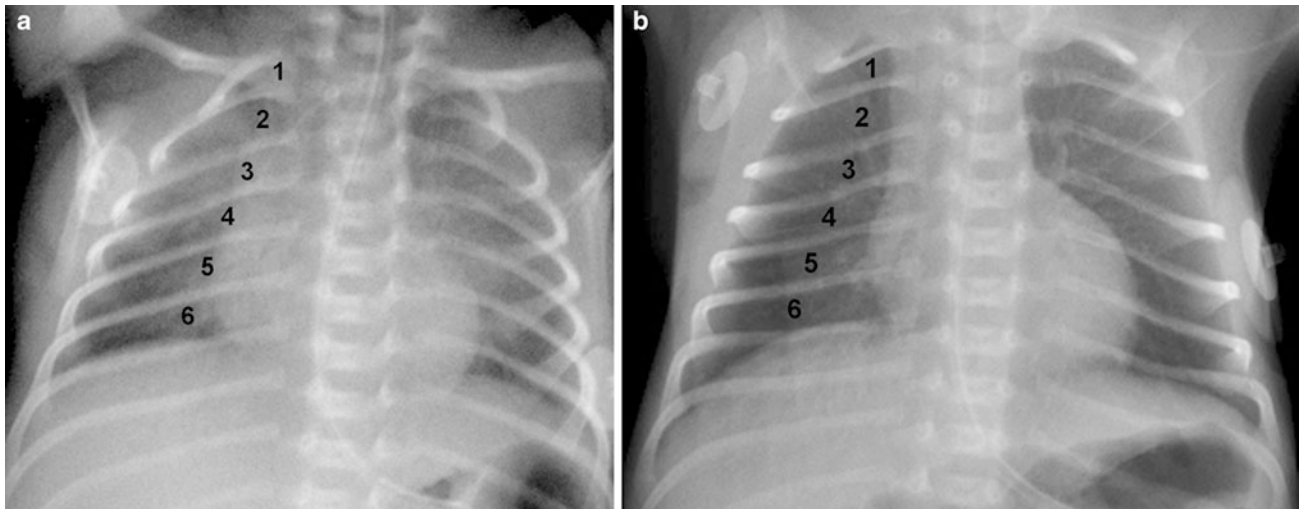
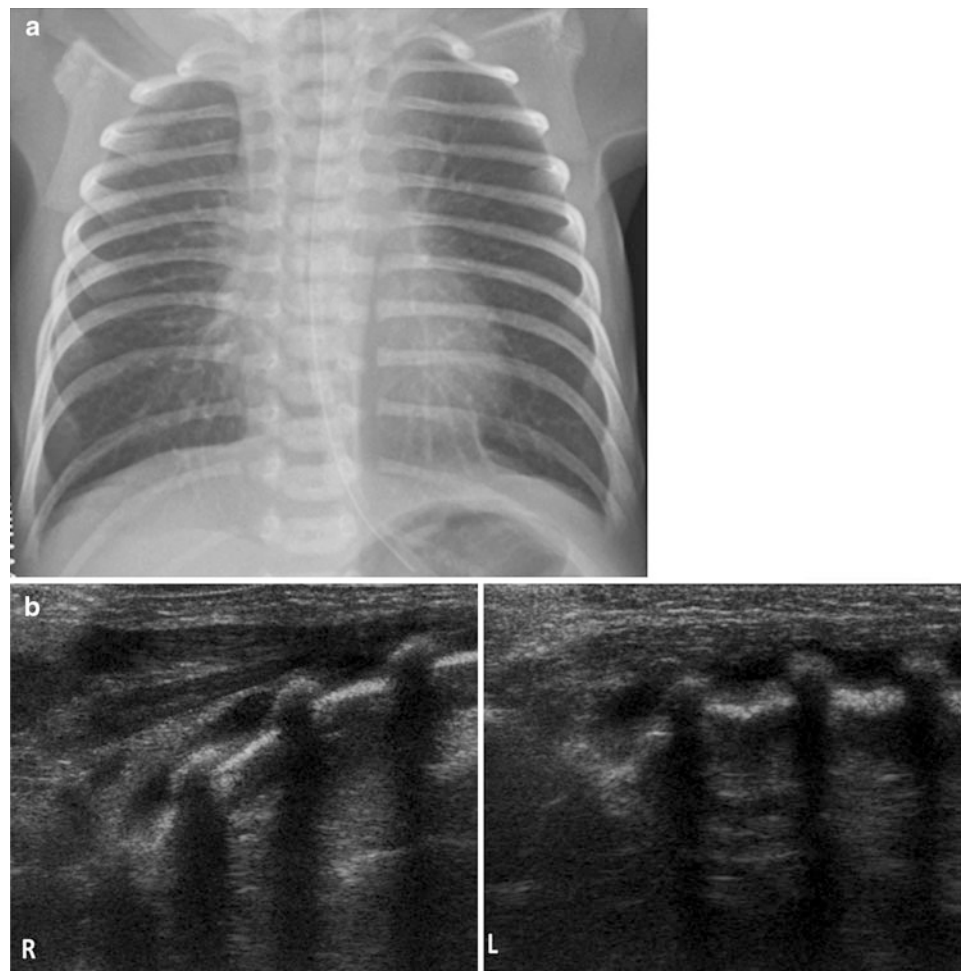


Fig. 21 Chest radiographs of an infant obtained during expiration (a) and inspiration (b). In both cases six intercostal spaces can be counted over the diaphragmatic dome. This method is unreliable to decide the phase in which the radiograph was obtained

Fig. 22 Poland Syndrome: apparent left lung hyperlucency due to hypoplasia of the left pectoralis major muscle. Note how the soft tissues of the left side of the chest wall are less dense and thinner than on the right side (a). Comparative US images of the chest wall show a very hypoplastic left pectoralis major muscle (b)



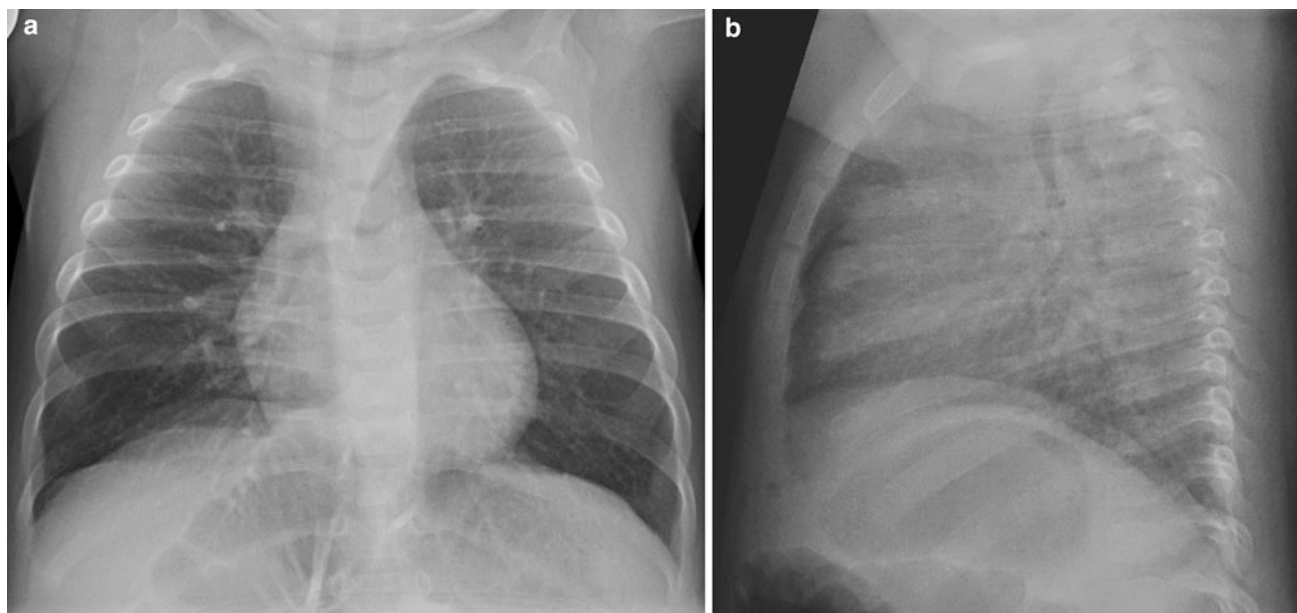


Fig. 23 Frontal (a) and lateral (b) chest radiographs of the same child obtained within minutes. The frontal view shows flattened hemidiaphragms but in the lateral view the diaphragms are in normal high position, which rules out air trapping

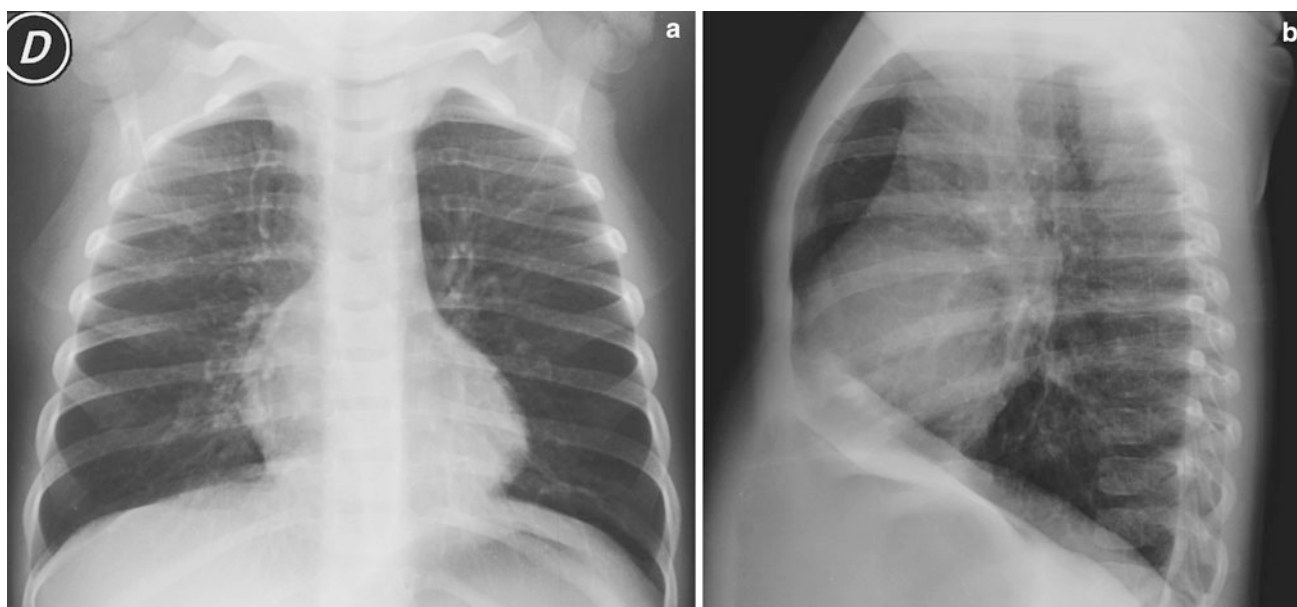


Fig. 24 Frontal (a) and lateral (b) chest radiographs of a child with bronchiolitis. Note also flattening of the diaphragm and a retrosternal lucency in the lateral view

Tetralogy of Fallot or isolated pulmonary artery stenosis, is the most frequent cause. Evaluation of the cardiovascular silhouette may be useful to suspect the underlying anomaly, but advanced cardiac imaging is needed to establish the final diagnosis.

3.2.2.4 Increased Lung Volume with Decreased Vascularity

Hyperlucent large lungs with decreased vascularity are characteristic finding of bronchiolitis obliterans, especially in advanced phases of the disease. Even if radiological



Fig. 25 Frontal chest radiograph of a child with foreign body aspiration. The left lung is large and hyperlucent with less vessels due to air trapping caused by partial obstruction of the left main bronchus. Note the mediastinal shift to the right

findings are subtle, severe obstructive involvement of pulmonary function may be present. CT is the modality of choice to establish the final diagnosis.

3.2.2.5 Unilateral Hyperlucent Lung

Unilateral hyperlucent lung is seen in a variety of pathologic conditions and careful analysis of the radiographic findings is necessary to make the correct diagnosis (Alford et al. 1993). Once technical pitfalls and extrapulmonary causes are excluded, the main challenge is to define if the

hyperlucent lung corresponds to the normal or the abnormal lung. Comparative evaluation of lung vascularity is the clue: in general terms the abnormal lung is the one that displays less vascularity. It is important to mention that the evaluation of number and size of lung vessels is subjective, and that expertise is important to correctly assess lung vascularity.

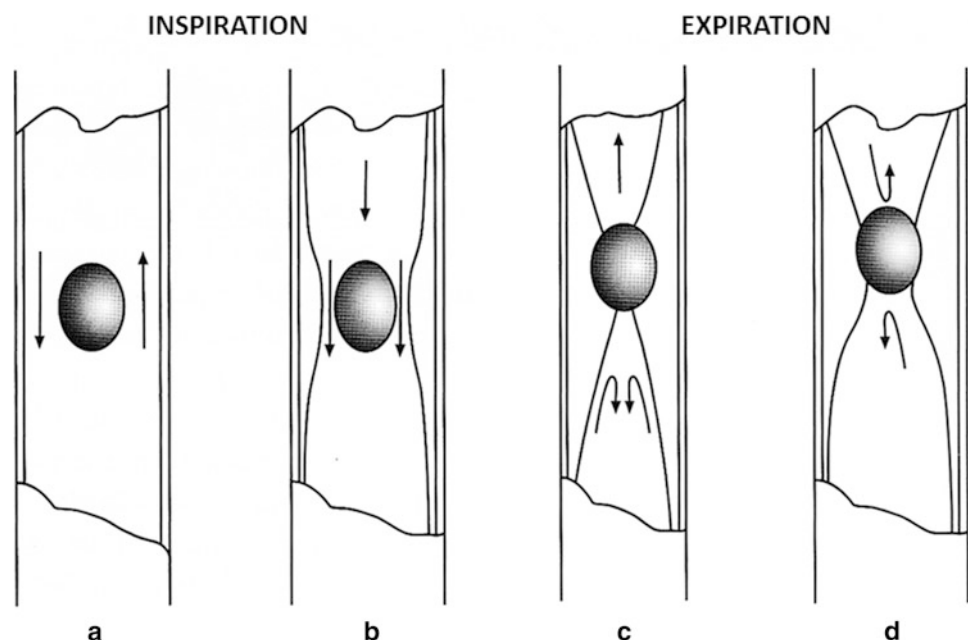
Aspiration of a foreign body is the more frequent pathologic cause of unilateral air trapping in children (Fig. 25). A two-way valve mechanism caused by partial bronchial obstruction causes air trapping during expiration (Fig. 26) (Kosucu et al. 2004; Alford et al. 1993). If radiologic findings are uncertain, expiratory images are of great help, as well as dynamic assessment of air trapping with fluoroscopy that will show mediastinal shift toward the contralateral side during expiration. It is important to mention that the history of choking, very useful for diagnosis, is not always present.

In a child with asymmetric lung transparency, usually the lung with less vascularity is the abnormal one.

Less frequently unilateral air trapping can be caused by extrinsic bronchial compressions, either vascular (e.g., pulmonary sling) or non-vascular (e.g., duplications cysts) (Alford et al. 1993). Similar findings can be seen with partially obstructive endobronchial tumors, which are extremely unusual in the pediatric age, being carcinoid the most frequent.

In Swyer James McLeod Syndrome, a predominantly unilateral bronchiolitis obliterans, the affected lung is hyperlucent and usually small (Fig. 27a, b). Lung hyperlucency is caused by air trapping due to small airway obstruction, and to the paucity of vascular structures in the affected parenchyma,

Fig. 26 Foreign body aspiration: Diagram of two-way valve mechanism and air trapping during expiration (Modified with permission from Moëgne and Ortega 2012)



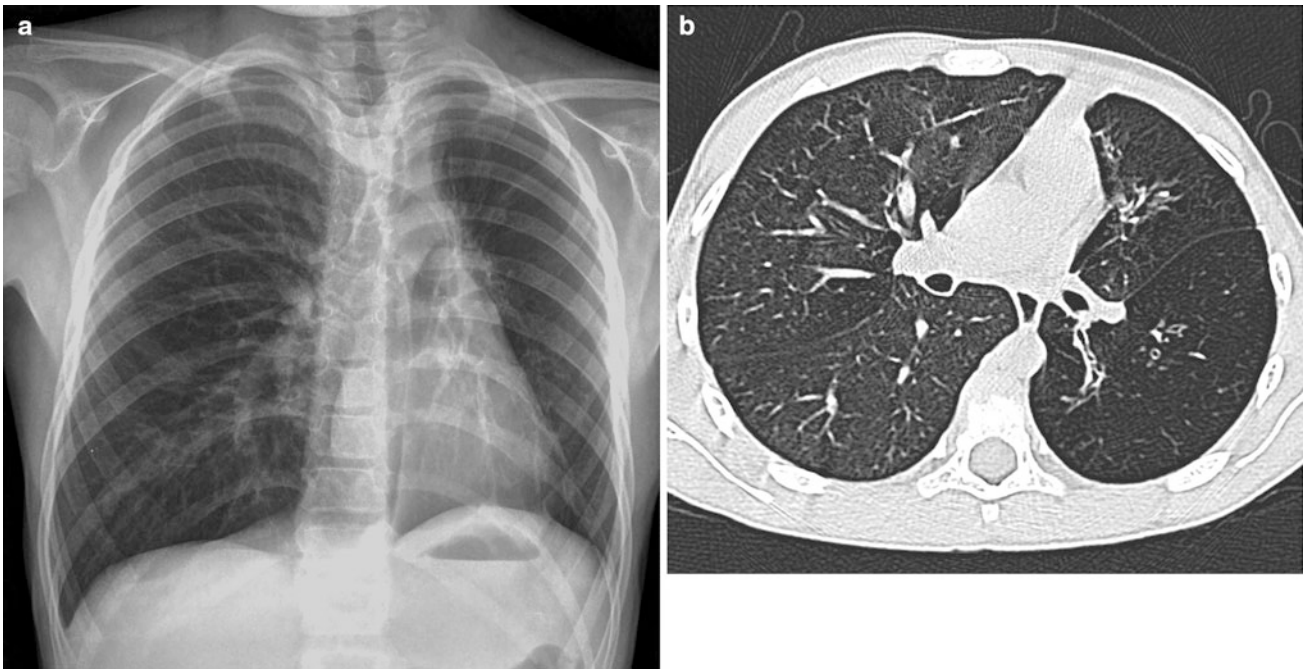


Fig. 27 Frontal chest X-ray (a) of a 3-year-old boy with a Swyer James Syndrome. Note small hyperlucent left lung and large compensatory right lung. High resolution CT (b) shows characteristic

findings of bronchiolitis obliterans in the left lung. In other images of this study small areas of mosaic pattern were seen in the right lung indicating bilateral, though very asymmetric, lung involvement

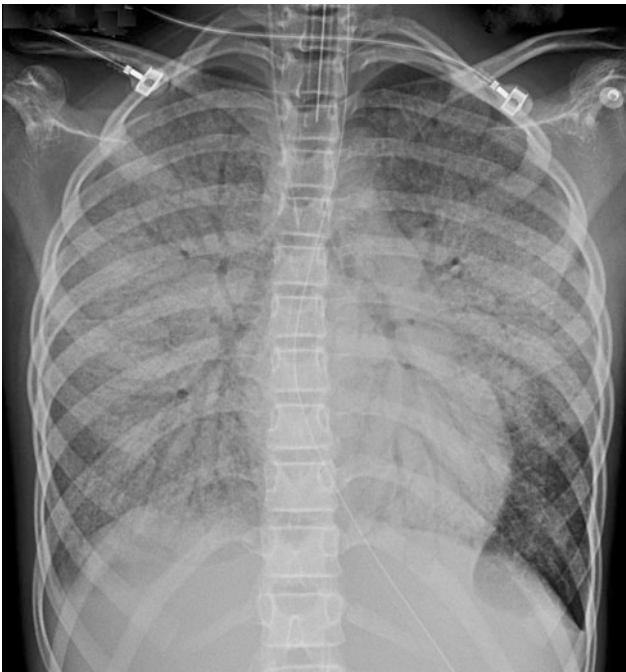


Fig. 28 Air bronchogram. Note the air within the bronchi surrounded by high-density alveolar spaces in this child with acute pulmonary distress syndrome

with redistribution of blood flow to less affected lung. The diagnosis is strongly suggested by radiological findings and has to be confirmed with CT (Kuhn and Brody 2002).

3.2.2.6 Increased Lung Density

Conditions that produce increased lung density are usually grouped according to the pulmonary space involved (Fraser 1996):

- Mainly air space involvement
- Mainly interstitial space involvement
- Involvement of both alveolar and interstitial spaces.

Air bronchogram is the classical radiological sign of alveolar space involvement. It represents air in patent airways surrounded by high-density alveolar spaces. This sign is frequent in consolidations and in atelectasis (Fig. 28). When air space involvement is less confluent, not well-defined nodular opacities, representing acinar involvement, are noted.

The silhouette sign occurs when the density of lung parenchyma is the same or greater than the density of adjacent mediastinum or diaphragm, resulting in loss of delineation of their contours (Fig. 29a, b). This is a useful sign to localize abnormalities, especially when a lateral view is not available, and it facilitates detection of subtle alterations that otherwise could be unrecognized.

Atelectasis is frequent in children because collateral air circulation through Kohn pores and Lambert channels is less efficient than in adults (Effmann and Kuhn 2004). Radiological signs of atelectasis are described in Table 1. The most reliable sign is displacement of inter-lobar fissures. Since the anterior and medium compartments of the mediastinum are

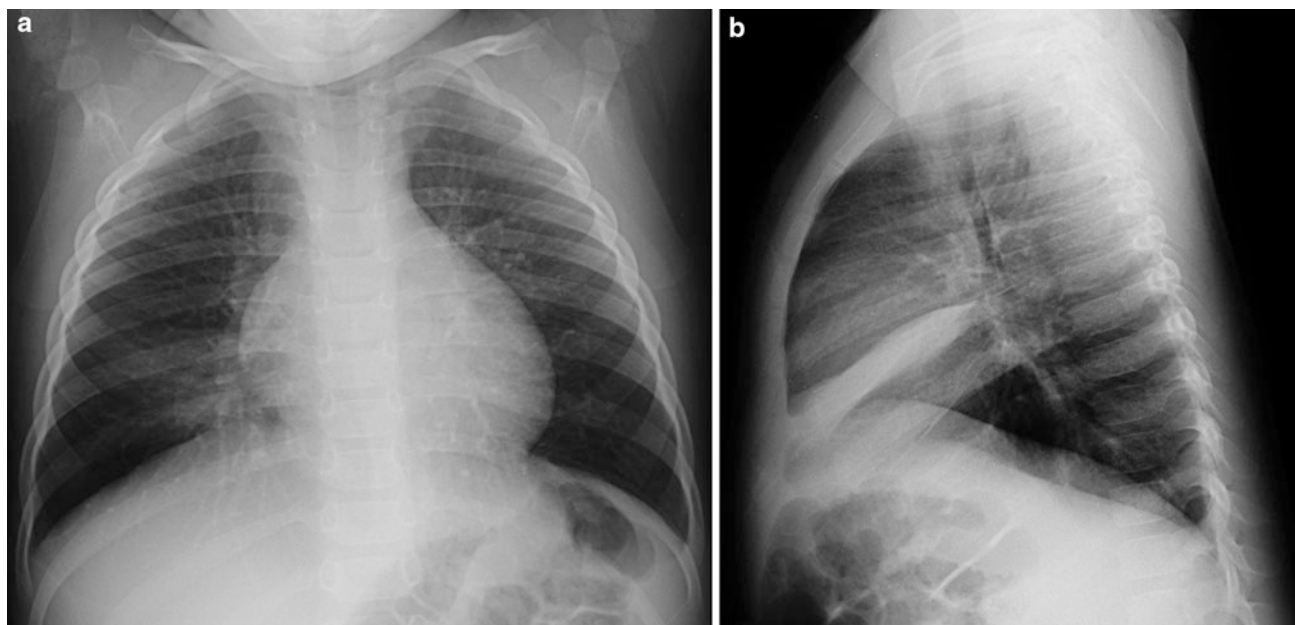


Fig. 29 Silhouette sign. In frontal view, an increased lung density in the right causes subtle loss of delineation of the cardiac border (a). Lateral view demonstrates atelectasis of the middle lobe (b)

Table 1 Radiological Signs of Atelectasis

Direct	Fissure displacement
Indirect	Increase of density
	Elevation of ipsilateral hemidiaphragm
	Ipsilateral mediastinal shift
	Smaller intercostal spaces
	Compensatory hyperinflation

less stable than the posterior compartment, and therefore displace more easily, it is frequent in atelectasis to note heart and thymus displacement, while the trachea remains in its normal position (Moënné and Ortega 2012).

3.2.3 Pleural Anomalies

Pleural effusion and pneumothorax are the main pleural abnormalities seen in children.

3.2.3.1 Pleural Effusion

When the equilibrium between the rate of entry and exit of pleural fluid and protein is lost, the result is pleural effusion (McLoud 1998). An increase of pleural fluid can be seen in infectious, inflammatory, traumatic, renal, cardiovascular, and tumoral conditions, and it can be either a transudate or an exudate, as shown in Table 2.

Even if chest radiographs have limited sensibility in detecting small effusions, it is the method by which pleural effusions are usually detected in children. Sensibility is even lower if the patient is imaged in supine position, especially in bilateral effusions (Fraser 1996).

Table 2 Types of effusions

Transudates	
Exudates	Empyema
	Hemothorax
	Chylothorax

US is the method of choice to characterize pleural effusions (Calder and Owens 2009) and helps to define the degree of therapeutic aggressiveness required for treatment (Donnelly 2005). Even if CT is highly sensitive in detecting small amounts of pleural fluid, it has a limited role in the evaluation of pleural effusions in children since it is less sensitive than US in demonstrating septums and loculi within the effusion (Donnelly 2005).

Gravity is the main force that determines fluid location within the pleural space. In standing position it initially locates between the diaphragm and the lung base from where it spills first to the posterior costophrenic sulcus, and then to the lateral costophrenic sulcus. Lateral views are important to detect small effusions since they show the posterior costophrenic sulcus, not seen on frontal views (Fig. 30). From the lateral costophrenic sulcus fluid ascends by capillarity through the pleural space, displaying a *Damoiseau curve* configuration (Fig. 31). Large pleural effusions can cause diffuse opacity of the hemithorax, with shift of the mediastinum to the contra lateral side. US is the method of choice to study the cause of an opaque hemithorax, showing the nature of the underlying disease.

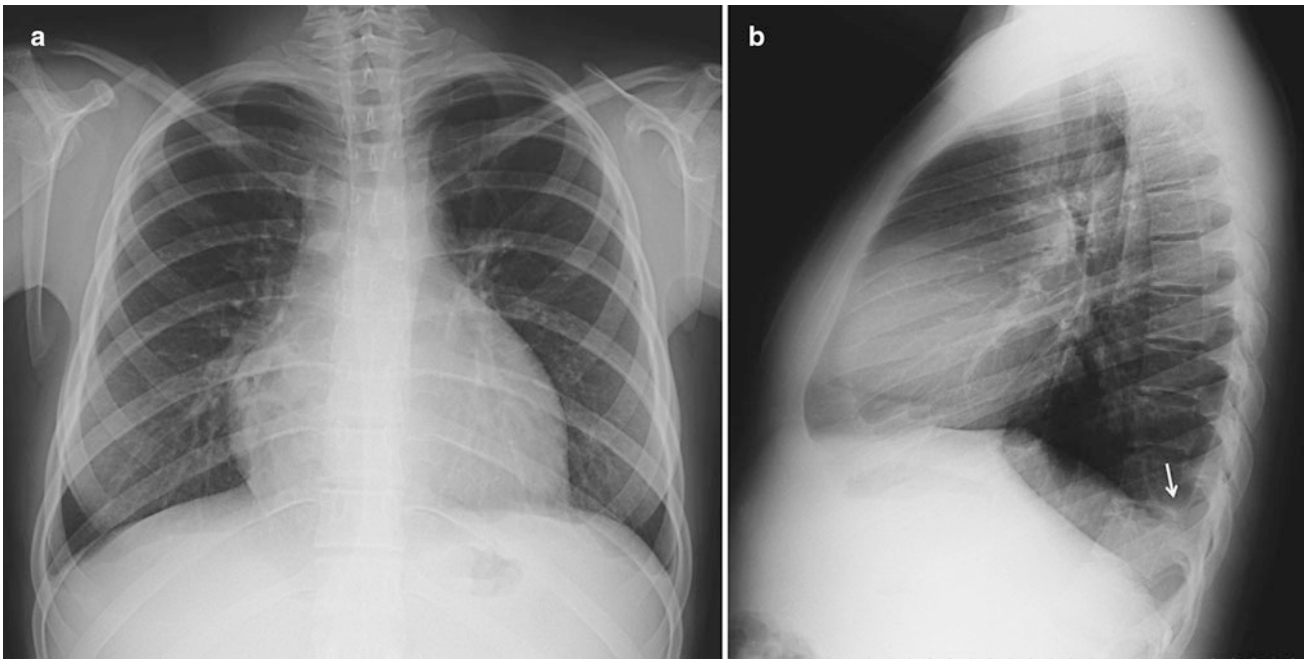


Fig. 30 Frontal (a) and lateral (b) chest radiographs in a child with a small left pleural effusion shown on the lateral view by demonstrating blurring of the posterior costophrenic sulcus (arrow)



Fig. 31 Left pneumonia with a large pleural effusion shows the characteristic Damoiseau curve configuration

Pleural effusions that collect in the subpulmonary space can be difficult to diagnose since in these cases the normal diaphragmatic shape is not lost, giving origin to the so-called “pseudo diaphragm” (Fig. 32). Table 3 shows the main radiological findings of subpulmonary pleural effusion.

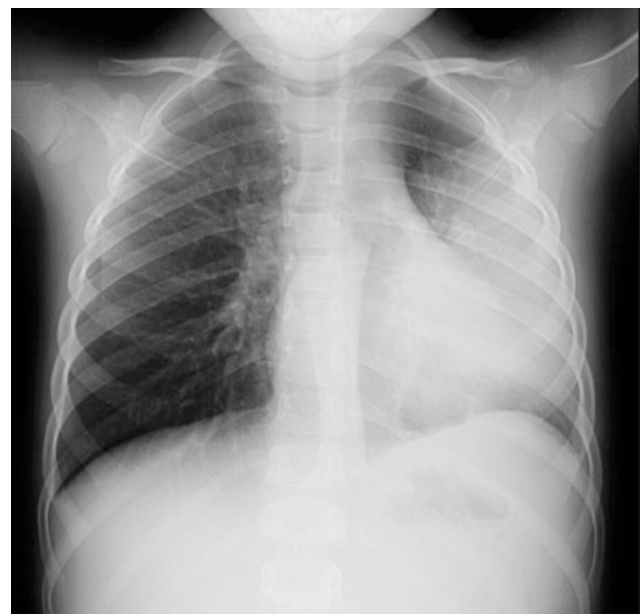


Fig. 32 Left pneumonia with a predominantly subpulmonary pleural effusion showing the characteristic findings described on Table 3

In supine position, fluid layers beneath the lung producing a homogeneous increase of radiological density. Small effusions may be difficult to recognize, especially if bilateral. When the amount of pleural fluid increases it extends to the lateral aspect of the pleural space causing a progressive pleural opacity adjacent to the lateral chest wall

Table 3 Radiological Signs of Subpulmonary Pleural Effusion

High position of the hemidiaphragm (“pseudo diaphragm”)
Lateralized dome of the “pseudo diaphragm” with a steep descent to the lateral costophrenic sulcus
Increase of the space between the “pseudo diaphragm” and the gastric fundus (left side effusions)
Lack of visualization of lung vessels through the diaphragm in frontal radiographs

(Fig. 33); eventually, the hemithorax will become diffusely opaque.

3.2.3.2 Pneumothorax

Air in the pleural space is always abnormal. It is caused by alveolar rupture secondary to trauma, lung air trapping, broncho-pulmonary fistula, pulmonary blebs, or barotrauma.

Identification of the “*free lung edge*,” which represents the visceral pleura delineated by air in the pleural cavity, is the classical sign of pneumothorax (Fig. 34). Variable degrees of adjacent lung atelectasis are usually present and in cases of tension pneumothorax mediastinum shift toward the contra lateral side will be present.

In standing position air initially surrounds the lung apex where the *free lung edge sign* will be first noted. In supine position free pleural air locates in the anterior-most part of the thoracic cavity, between the lung and the thoracic cage. If the amount of air is small it will not extend to the lateral aspect of the pleural cavity, and the *free lung edge sign* will



Fig. 34 Right pneumothorax with visualization of the visceral pleura delineated by the air within the pleural cavity (“*free lung edge*” sign). Ipsilateral atelectasis flattening of the hemidiaphragm and mediastinal shift are also present

not be present, making the diagnosis more challenging. Several subtle radiological findings are useful to diagnose an anterior pneumothorax (Fig. 35):

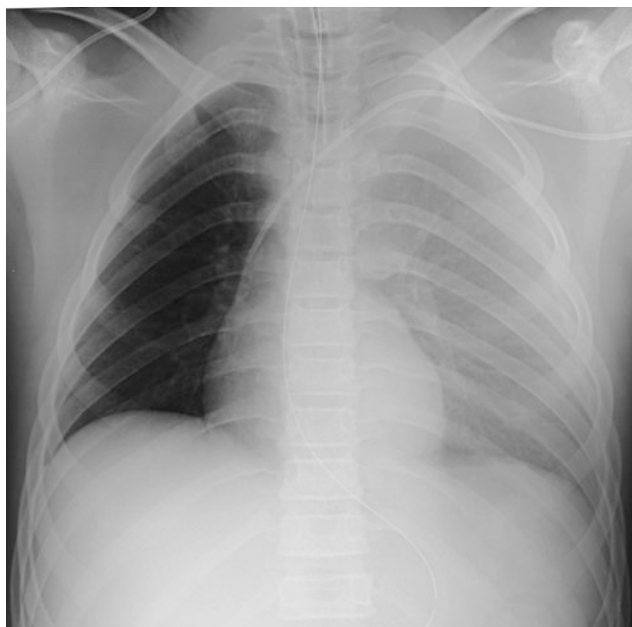


Fig. 33 Frontal chest radiograph obtained in supine showing increase in density of the left hemithorax caused by pleural fluid layered under the lung



Fig. 35 Predominantly anterior right pneumothorax. The right hemithorax is hyperlucent and shows the “*deep lateral costophrenic sulcus*” sign

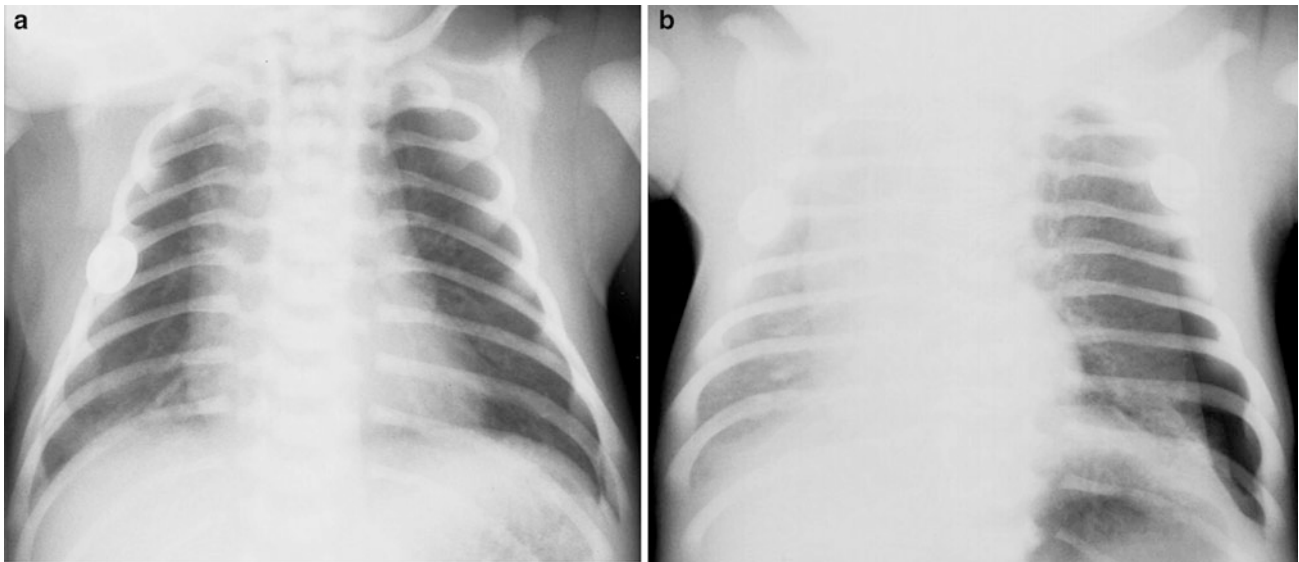


Fig. 36 Frontal chest radiograph. (a) shows subtle left hemithorax hyperlucency and mediastinal shift, in a newborn. An expiratory view. (b) shows air in the pleural space and the “free lung edge” sign



Fig. 37 At the right side, a skin fold may be misinterpreted as a pneumothorax. Note that the line extends outside of the chest wall

- Hyperlucent hemithorax
- Increased definition of the mediastinum border
- Deep lateral costophrenic sulcus (Gordon 1980).

In children with uncertain findings, a cross-table lateral image or an expiratory radiograph can be useful to demonstrate the free pleural air (Fig. 36a, b).

A frequent pitfall, especially in newborns and small infants, is the interpretation of a skin fold as the *free lung edge sign*. The clues to properly recognize skin folds are to look for lung vessels between it and the thoracic wall, and to search for its extension to the soft tissues, beyond the border of the lung (Fig. 37).

4 Conclusion

Knowledge of the classical radiological findings as well as of the most frequent technical pitfalls is mandatory to interpret correctly chest radiographs in children and make correct diagnoses.

References

- Alford B, McIlhenny J, Silen M et al (1993) Asymmetric radiographic findings in the pediatric chest: approach to early diagnosis. *Radiographics* 13:77–93
- Bramson RT, Griscom NT (2005) Interpretation of Chest Radiographs in Infants with Cough and Fever 236(1):22–29
- Calder A, Owens C (2009) Imaging of parapneumonic pleural effusions and empyema in children. *Pediatr Radiol* 39:527–537
- Chalumeau M, Le Clainche L, Sayeg N et al (2001) Spontaneous pneumomediastinum in children. *Pediatr Pulmonol* 31:67–75
- Chang L, Lee F, Gwinn J (1970) Normal lateral deviation of the trachea in infants and children. *AJR* 109:247–251
- Donnelly L (2005) Imaging in immunocompetent children who have pneumonia. *Radiol Clin N Am* 43:253–265
- Effmann E, Kuhn J (2004) Lung and airways chap I part II in Caffey's pediatric diagnostic imaging. Mosby, Philadelphia, pp 891–898

- Enríquez G, García-Peña P, Lucaya J (2009) Pitfalls in chest imaging. *Pediatr Radiol* 38(Suppl 3):S356–S368
- Fefferman N, Pinkney L (2005) Imaging evaluation of chest wall disorders in children. *Radiol Clin N Am* 43:355–370
- Fraser R (1996) El tórax normal: sinopsis de las enfermedades del tórax. Marban, Madrid, Cap 1, pp 79–88
- Frush D, Donnelly L, Chotas H (2000) Contemporary pediatric thoracic imaging. *AJR* 175:841–851
- Gordon R (1980) The deep sulcus sign. *Radiology* 136:25–27
- Han B, Yoon H, Suh Y (2001) Thymic ultrasound I. Intrathymic anatomy in infants. *Pediatr Radiol* 31:474–479
- Kosucu P, Ahmetoglu A, Koramaz I et al (2004) Low-dose MDCT and virtual bronchoscopy in pediatric patients with foreign body aspiration. *AJR* 183:1771–1777
- Kuhn J, Brody A (2002) High-resolution CT of pediatric lung disease. *Radiol Clin N Am* 40(1):89–102
- Kuhn J, Effmann E (2004) Overview of imaging procedures in the pediatric neck and thorax. In: Caffey's pediatric diagnostic imaging, Mosby, Pensilvania, Sección IV, part I, 767–776
- McLoud T (1998) The pleura in thoracic radiology: The requisites, Mosby, Missouri, Chap 18, 483–513
- Moëne K, Ortega X (2012) Diagnóstico por imágenes del tórax pediátrico. Segunda edición. Buenos Aires, Ediciones Journal
- Nasseri F, Eftekhari F (2010) Clinical and radiologic review of the normal and abnormal thymus: pearls and pitfalls. *Radiographics* 30:413–428. Published on line doi:[10.1148/rg.302095131](https://doi.org/10.1148/rg.302095131)
- Salour M (2000) The steeple sign. *Radiology* 216:2 428–429
- Swischuk L (1997) Respiratory system, chap 1 in imaging of the newborn, infant and young child. Williams and Wilkins, Maryland, pp 1–158
- Swischuk L (1971) Anterior tracheal indentation in infancy and early childhood: normal or abnormal? *AJR* 112:12–17
- Zylak C, Standen J, Barnes G et al (2000) Pneumomediastinum revisited. *Radiographics* 20:1043–1057

Pediatric Chest Imaging

Garcia-Peña, P.; Guillerman, R.P. (Eds.)

2014, IX, 545 p. 900 illus., 100 illus. in color., Hardcover

ISBN: 978-3-642-37336-7